Hindawi
Advances in Civil Engineering
Volume 2023, Article ID 2869772, 13 pages
https://doi.org/10.1155/2023/2869772

Research Article

Experimental Study of Single Structure Surface Dangerous Rock Mass Dynamic Characteristics Based on Constant Micromotion

Anchi Shi,[1,2] Mowen Xie,[3] Liuyuan Zhao,[1,2] Xiaoyong Zhang,[3] Zhixiang Wu,[3] and Simiao Wu[3]

[1]*PowerChina Huadong Engineering Corporation Limited, Hangzhou, Zhejiang 311122, China*
[2]*Zhejiang Huadong Construction Engineering Corporation Limited, Hangzhou, Zhejiang 310004, China*
[3]*School of Civil and Resource Engineering, University of Science and Technology Beijing, Beijing 100083, China*

Correspondence should be addressed to Mowen Xie; mowenxie@126.com

Received 1 April 2023; Revised 3 May 2023; Accepted 4 May 2023; Published 20 May 2023

Academic Editor: Suraparb Keawsawasvong

The dynamic parameters of a dangerous rock mass reflect the degree of damage of the structure of its surface. There is still an urgent problem to identify the dynamic parameters of a dangerous rock mass based on the characteristics of the constant micromotion at its site. To address this problem, a method is proposed to identify the dynamic characteristics of a dangerous rock mass undergoing excitation caused by constant micromotion: (1) the vibration of a dangerous rock mass undergoing excitation from constant micromotion is classified as forced undamped structural vibration with a single degree of freedom. The ratio of the amplitude of the spectrum of the dangerous rock mass to the amplitude of the spectrum of the bedrock is defined as the relative amplitude spectrum. The first-order natural frequency is identified from the relative amplitude spectrum. (2) Bedrock is the source of excitation of a dangerous rock mass. When a mechanical wave propagates to a dangerous rock mass, it crosses the porous surface of media with structural damage, and mechanical wave scattering occurs. The frequency domain of the mechanical wave changes. The center frequency shifts to a low frequency. By means of laboratory model tests, the changes in the dynamic parameters of models of a cantilevered dangerous rock mass and a sliding dangerous rock mass with structural surface damage are analyzed. It is concluded that (1) based on the theory of vibration mechanics, the first-order natural frequencies of dangerous rock masses can be obtained from their relative amplitude spectra. The first-order natural frequencies of dangerous rock masses undergoing constant micromotion are measurable. (2) The damage of the structural surface of a dangerous rock mass with macroscopic fractures can be identified by its first-order natural frequency. The center frequency cannot reflect the development of fractures. The damage of the structure of the surface of a dangerous rock mass with microscopic fractures can be identified by the change in the center frequency in its high-frequency band. The first-order natural frequency cannot reflect the development of fractures. (3) There are limitations in using single vibration mechanics theory or elastic wave scattering theory to analyze the damage of the structure of the surface of a dangerous rock mass; it is more effective to integrate both methods.

1. Introduction

The collapse of a dangerous rock body is a geological phenomenon in which a rock body suddenly breaks from the collapse of the parent rock body under the action of gravity and natural power. It brings a great threat to the safety of people's lives and property in society. There are many external factors that lead to the destabilization and collapse of dangerous rock masses, such as weathering, rainfall, earthquakes, or freezing. These factors lead to the destruction of rock bridges, which reduce the strength of the surface structure and eventually lead to the destabilization and collapse of dangerous rock masses [1]. Studies have shown that the decrease in stability of dangerous rock masses is mainly controlled by the strength of the surface structure [2]. According to the form of damage of a dangerous rock mass and the damage characteristics of the structure of its face, dangerous rock masses can be classified as sudden dangerous rock masses and progressive dangerous rock masses [3]. The destabilization and collapse of

a dangerous rock mass can be analyzed in terms of environmental indicators, displacement indicators, and dynamic characteristics. Environmental indicators are mainly analyzed from the aspects of climate, water environment, weathering, and earthquakes. The means of displacement analysis are mainly the total station, oblique meter, multipoint displacement meter, seismometer, global positioning system (GPS), three-dimensional laser scanning (TLS), interferometric radar technology (INSAR), close-up photogrammetry (CRP), distributed optical fiber sensing (DOFS), and so forth [4–8]. The analysis of dynamic characteristics is based on the theory of damage structure dynamics and applied to analyze the destabilization process of dangerous rock masses [9–13]. A series of laboratory experiments by Du et al. [14] showed that the precursor damage characteristics of dangerous rock masses could be identified by their natural frequencies. Natural frequencies have obvious advantages over other indicators. Based on this, a dynamic indicator monitoring system was established that can play a positive role in the monitoring of the loss and destruction of dangerous rock bodies. Through theoretical calculations and experiments, Zhang et al. [15, 16] proved that the stability of a hazardous rock body has a strong correlation with its inherent vibration frequency. Xie et al. [17] proposed a method to calculate the stability coefficient of a dangerous rock mass based on its natural frequency. The response to environmental vibration also has some connection with the stability of a dangerous rock mass. Bottelin [18] monitored the frequency of a columnar limestone mass before and after reinforcement and found that the natural frequency was greater after reinforcement.

At present, the analysis of the stability of dangerous rock masses based on dynamic characteristics is still in the experimental stage [19]. Experiments are mostly performed by manually tapping to motivate and measure dynamic feature parameters of dangerous rock masses. In actual engineering, dangerous rock masses are often located on high and steep slopes, and it is dangerous to climb to the location of a dangerous rock masses to excite it. Dangerous rock masses are often large in volume, and it is difficult to determine the strength of an artificial excitation. Therefore, manual tapping is not practical. In practice, micromotions are imperceptible to humans at any location in any region on the Earth's surface at all times [20]. Such micromotions are formed by the joint action of various vibration sources in all directions, and they are called constant micromotions. Constant micromotions carry information about the characteristics of the vibration during propagation at a site. They are often used in seismic testing at sites [21, 22]. Constant micromotion is a natural source of vibration, and thus, it can be considered the source of excitation of a dangerous rock mass. This paper mainly studies a theoretical model for the undamped vibration with a single degree of freedom of the structure of a dangerous rock mass under constant micromotion, and it deduces a method for the calculation of the first-order natural frequency and a principle for the analysis and measurement of the center frequency. Additionally, this paper analyzes the application of experimental models to both cantilevered dangerous rock masses and sliding dangerous rock masses. This paper also provides a set of methods for monitoring the structure of the surface of a single dangerous rock mass to provide a useful reference for the automated monitoring of dangerous rock masses.

2. Research on the Identification of the Dynamic Characteristic Parameters of a Dangerous Rock Mass Based on Constant Micromotion

2.1. Introduction to a Dangerous Rock Mass Controlled by a Single Surface Structure. According to the fracture morphology of the surface structure of a dangerous rock mass, a rock mass can be classified as controlled by macroscopic or microscopic fracture [23–25]. A cantilevered dangerous rock mass is a typical example of a dangerous rock body controlled by macroscopic fracture. A sliding dangerous rock body is a typical example of a dangerous rock body controlled by microscopic fracture, as shown in Figure 1.

As shown in Figure 1(a), the cantilevered dangerous rock mass is a pull-apart dangerous rock mass. The vertical joints of the rock structure are well developed, and the bottom surface of the dangerous rock mass is empty and unsupported. The shape of the dangerous rock mass is similar to a horizontal beam or a longitudinal beam cantilevered on bedrock. The bonding surface of the dangerous rock mass and the bedrock is mainly subjected to the compound tension-shear force caused by self-weight. The damage of the dangerous rock mass is mainly manifested by the formation of macroscopic fractures at the trailing edge and the partial separation of the dangerous rock mass from the lateral bedrock. When macroscopic fractures continue to develop until the force is greater than the strength of the main control bond surface, the rock bridge fractures, and the dangerous rock mass collapses [26]. As shown in Figure 1(b), unlike the cantilevered dangerous rock mass, the sliding dangerous rock mass slope mass has surface structure outside the steeply inclined slope. The bonded surface of the dangerous rock mass and the bedrock is mainly subject to the shear force caused by self-weight. Dangerous rock mass damage is mainly manifested as the development of microscopic fractures on the structural surface and decreases in cohesion and internal friction angle. During this period, there is often no macroscopic fracture, and the dangerous rock mass and bedrock basically remain in a fit state before the damage [27–29].

2.2. First-Order Natural Frequency Analysis of Dangerous Rock Masses

2.2.1. First-Order Natural Frequency Identification Principle. The generation of constant micromotion can be divided into two categories: natural factors and human factors. The former consists of wind, rain, waves, volcanic activity, and so forth. The latter includes factory production, transportation, building construction, and so forth. Constant micromotion is caused by the collection of various vibration sources in all directions. This natural frequency of microvibration is a collection of vibrations in various frequency bands or white

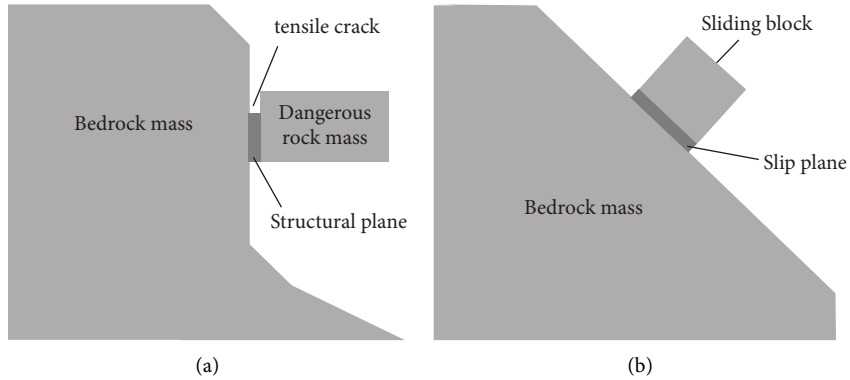

Figure 1: Schematic diagrams of dangerous rock masses controlled by a single structural plane: (a) cantilevered dangerous rock mass and (b) sliding dangerous rock mass.

noise. When the vibration of a certain frequency band of microvibration is close to the natural frequency of the dangerous rock mass, the vibration of this frequency band causes resonance with the dangerous rock mass [30].

For a dangerous rock mass, its first-order natural frequency is the easiest index to identify [3, 15, 16, 19]. Therefore, this study focuses on the first-order natural frequency of the dangerous rock mass. On this basis, if we focus only on the first-order natural frequency, then the problem of a dangerous rock mass with multiple degrees of freedom is transformed into a problem with a single-degree-of-freedom. Under the condition of constant micromotion, the energy required for vibration is continuously transferred from the bedrock to the dangerous rock. Therefore, the dangerous rock mass is forced to vibrate. In addition, the damping condition of the dangerous rock mass is considered to be undamped. Taking the above considerations into account, the problem of identifying the first-order natural frequency of the dangerous rock mass is regarded as the problem of the forced vibration of a structure with a single degree of freedom under the undamped condition of the dangerous rock mass.

The equation of forced vibration of a system with a single degree of freedom is given by

$$-\mathrm{kx} - c\frac{\mathrm{dx}}{\mathrm{dt}} + F_d = m\frac{\mathrm{d}^2x}{\mathrm{dt}^2}, \tag{1}$$

where k is the spring system stiffness; c is the viscous damping; F_d is the driving force of the simple harmonic vibration, $F_d = F_0 \cos \omega_d t$.

From the differential equation, the amplitude $A_b(t)$ of the dangerous rock mass under steady-state vibration conditions can be solved

$$A_b(t) = \frac{F_0}{k}\frac{1}{\sqrt{\left(1-\lambda^2\right)^2 + (2\xi\lambda)^2}}\sin\left(\omega_d t + \varphi\right), \tag{2}$$

where $\lambda = \omega_d/\omega_0$; $\omega_0 = \sqrt{k/m}$; $\xi = c/2m\omega_0$; ξ is the damping ratio; and φ is the phase angle.

From equation (2), we can obtain the ratio of the acceleration of the dangerous rock mass to the acceleration of the vibration source:

$$K = \left|\frac{d^2A_b/\mathrm{dt}^2}{F_0/m}\right| = \frac{1}{\sqrt{\left(1-\lambda^2\right)^2 + (2\xi\lambda)^2}} \approx \frac{1}{1-\lambda^2}. \tag{3}$$

Equation (3) shows that below the resonant frequency point, the ratio of the spectrum amplitude of dangerous rock and the bedrock acceleration is greater than 1, and the nonresonant frequency point is less than or equal to 1. According to this property, the first-order natural frequency can be evaluated. The ratio of the amplitude of the spectrum of the dangerous rock mass to the amplitude of the spectrum of the bedrock–frequency curve is defined as the relative amplitude spectrum.

2.2.2. Design of the First-Order Natural Frequency Measurement Method. Due to the large amount of noise and complex excitation contained in a constant micromotion, the direct Fourier transform of vibration data can cause problems such as false modes, real mode omission, and computational efficiency. The Welch method [31] can be used to effectively suppress random noise in data and obtain the vibration power spectrum. The amplitude of the power spectrum is the square of the amplitude of the Fourier spectrum. Based on this relationship, a power spectrum can be converted to a Fourier spectrum. In turn, the spectrum of bedrock and dangerous rock mass can be effectively calculated. As shown in Figure 2, the first-order natural frequencies of a dangerous rock mass with a single surface structure are measured as follows:

(1) Step (1): The power spectra of the dangerous rock mass and bedrock vibration are obtained based on the Welch method and then convert them into frequency spectra

(2) Step (2): The relative amplitude spectrum is calculated through the ratio of the amplitude of the spectrum of the dangerous rock mass and the amplitude of the spectrum of the bedrock

(3) Step (3): According to the relative amplitude spectrum, the frequency point corresponding to the largest point of the relative amplitude is selected as

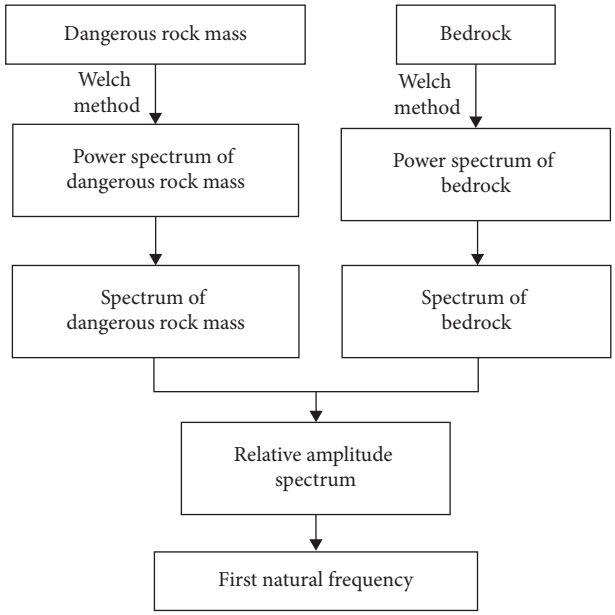

Figure 2: Identification process of the first-order natural frequency of a dangerous rock mass.

the first-order natural frequency of the dangerous rock mass

2.3. Dangerous Rock Mass Center Frequency Analysis

2.3.1. Elastic Wave Scattering Theory. In elastic dynamic problems, sometimes, it is necessary to examine vibrational phenomena, and sometimes, it is necessary to study fluctuating processes. There are two corresponding mathematical forms of their solutions: oscillatory and fluctuating. The wave solution has the form of a traveling wave, which can describe the fluctuation process visually and graphically. The vibration solution is usually an infinite number of steps, each of which represents a standing wave vibrating at a certain frequency. There is an intrinsic connection between the propagation fluctuations of elastic waves and the vibrations of elastomers, which can be seen as different manifestations of the same physical problem. For a dangerous rock mass with relatively small geometry, it is simpler and more feasible to analyze it directly as a vibration problem, which means that the damage to the surface structure can be analyzed by the first-order natural frequency of the rock mass. However, it is more reasonable to treat the parts of the medium of the object, such as internal holes and fractures, under dynamic loading as fluctuation problems. By analyzing the wave bypassing and scattering processes when passing through the obstacle, the changes in these parts can be described in detail. Therefore, it is necessary to analyze the development of microscopic fractures on the structural surface of dangerous rock masses by means of elastic wave scattering theory.

According to the characteristics of elastic wave propagation, there is a scattering phenomenon of elastic wave propagation in porous damaged solid media. The larger and more numerous the characteristic size of microscopic fractures are, the more severe the scattering is, especially in the high-frequency part of the elastic wave [32–34]. Due to the scattering of elastic waves at microfractures, their high-frequency elastic wave energy is attenuated. The structural plane damage is mainly developed in the interior of the critical rock body, so it is more appropriate to use the bulk wave for analysis. The bulk wave contains S-wave and P-wave, both of which can be applied to damage identification. In this study, S-wave was used for analysis. To analyze the changes in the high-frequency component characteristics of elastic waves, this paper uses the center frequency index to characterize the high-frequency frequency band characteristics of the dangerous rock mass. The center frequency is calculated as follows:

$$F = \frac{\sum_{f_0}^{f_m} f_k A_k}{\sum_{f_0}^{f_m} A_k}, \tag{4}$$

where $f_0 \sim f_m$ is the high-frequency range analyzed, f_k is the frequency value, A_k is the corresponding amplitude of f_k, and F is the center frequency value.

As the damage process of the dangerous rock mass depends on the form and degree of damage, its first-order natural frequency may also change. When the frequency range of the center frequency calculation includes the first-order natural frequency, the center frequency changes with the change in the first-order natural frequency. Therefore, to make the center frequency only reflect scattering phenomena when an elastic wave propagates in the porous damage solid medium, the selected high-frequency starting frequency f_0 should be greater than the first-order natural frequency of the dangerous rock mass.

2.3.2. Design of the Center Frequency Measurement Method. In the design of the first-order natural frequency measurement method of the dangerous rock mass, the spectra of the dangerous rock mass and the bedrock are obtained, and the center frequency of the dangerous rock mass can be calculated by equation (4). As shown in Figure 3, the first-order natural frequency measurement method for a dangerous rock mass with single surface structure is as follows:

(1) Step (1): The power spectra of the dangerous rock mass and bedrock vibration are obtained based on the Welch method and then convert them into frequency spectra

(2) Step (2): The high-frequency range above the first-order natural frequency of the dangerous rock mass and bedrock is selected

(3) Step (3): The center frequency of the dangerous rock mass and bedrock from the center frequency calculation formula is obtained

3. Laboratory Experiments

For the abovementioned first-order natural frequency identification method, we verify its feasibility by using two kinds of models of dangerous rock mass, cantilevered dangerous rock masses, and sliding dangerous rock masses.

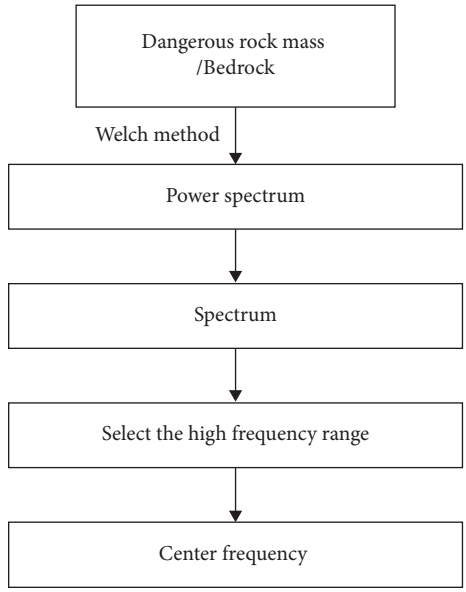

Figure 3: Calculation process of the center frequency of the dangerous rock mass.

3.1. Introduction of Experimental Model and Equipment

3.1.1. Model Size and Material. Based on the relative scale characteristics of the mountain bedrock and the dangerous rock mass, the size of the bedrock model was designed to be larger than the dangerous rock mass model. An electro-hydraulic servo-loading system was used to fix the bedrock in the experiment. In this way, the bedrock-dangerous rock system was closer to the actual situation, and the influence of size effect was reduced. Therefore, the design was as follows:

(1) The dimensions of the bedrock model of the cantilevered dangerous rock mass were 30 cm in length, 30 cm in width, and 30 cm in thickness; the dimensions of the dangerous rock mass model were 12 cm in length (*Y*-direction) *L*, 11.5 cm in width (*X*-direction) B, and 9.5 cm in thickness (*Z*-direction) H, as shown in Figure 4(a). (2) The dimensions of the bedrock model of the dangerous sliding rock mass were 50 cm in length, 30 cm in width, and 25 cm in thickness; the dimensions of the dangerous rock mass model were 7 cm in height (*Y*-direction) H, 7 cm in width (*X*-direction) B, and 7 cm in thickness (*Z*-direction) *L*, as shown in Figure 4(b).

The model material ratios and physical property parameters are shown in Tables 1 and 2.

3.1.2. Introduction of Vibration Acquisition Equipment. The test used the DASP modal test system to collect the vibration acceleration data of the dangerous rock mass model. The DASP modal test system mainly included an INV3062C signal collector, an INV9832-50 acceleration sensor, an excitation hammer, and other equipment. The signal acquisition instrument and acceleration sensor are shown in Figure 5, and the technical parameters of the equipment are shown in Tables 3 and 4, respectively.

3.2. Test Procedure

3.2.1. Cantilevered Dangerous Rock Mass. To simulate the changes in dynamic parameters due to the changes in crack depth at the trailing edge of the dangerous rock mass, cracks were cut at the trailing edge of the dangerous rock mass model. The depth of each crack was 1 cm, as shown in Figure 6. Each time after a crack was cut, the rock was left to stand for 1 minute, and then vibration data were collected. During the data acquisition process, no artificial excitation was applied to the dangerous rock mass model, and the main excitation came from constant micromotion. The vibration sampling frequency was 4000 Hz. During this experiment, the cantilevered dangerous rock mass model was cut until it was destabilized, and a total of 6.5 cm of cracks were cut on the trailing edge of the cantilevered dangerous rock mass model.

3.2.2. Sliding Dangerous Rock Mass. The dangerous rock mass and slip plane of real rock mass materials are difficult to build. Considering that the basic laws of elastic wave scattering in porous media of different materials are consistent, this test used other materials to simulate the sliding dangerous rock mass model. To simulate the damage process of the bonding surface of the sliding dangerous rock mass, water-soluble glue was used to bond the dangerous rock mass model to the bedrock model [35–37]. Then, it was placed outdoors for 24 hours at −2~−10°C to freeze the water-soluble glue between the model and the bedrock model. The surface of frozen ice was used as the bonding surface between the dangerous rock mass and the bedrock. The process of changing the surface from freezing to melting was compared to the process of bonding the surface from integrity to damage, as shown in Figure 7. During the freezing and melting of the surface, no artificial excitation was applied to the dangerous rock mass model. Vibration

(a) (b)

Figure 4: Experimental models: (a) cantilevered dangerous rock mass model and (b) sliding dangerous rock mass model.

Table 1: Model material ratio.

Component	Mass proportion (kg)
Quartz sand	50
Blanc fixe	30
Gypsum	8
Retarder	0.02
Water	10
Glycerol	1.5

Table 2: Model material properties.

Material properties	Cantilever dangerous rock mass model	Sliding dangerous rock mass model
Density ($kg{\cdot}m^{-3}$)	2230	2502
Elastic modulus (GPa)	2.4	3.01
Poisson ratio	0.28	0.30
Tensile strength (MPa)	0.0975	—
Cohesion (MPa)	0.926	—

Note. Due to the change in time and operators in the two experimental model castings, the physical properties of the model materials were different.

(a) (b)

Figure 5: Testing equipment: (a) signal acquisition instrument and (b) acceleration transducer.

acceleration data were collected every 1 minute under the condition of constant micromotion, the acquisition duration was 1 minute, and a total of 25 sets of data were collected. The sampling frequency of the acceleration collector was set to 4000 Hz, and the dangerous rock mass model was not displaced throughout the experiment.

3.3. Analysis of Experimental Results

3.3.1. Cantilevered Dangerous Rock Mass

(1) First-Order Natural Frequency. The first-order natural frequencies in the *Z*-direction were mainly considered for

Table 3: Technical parameters of the signal acquisition instrument.

Technical parameters	Parameter
Precision	24 bit $\Delta - \sum$ AD
Frequency range (Hz)	0.6~216 k
Range (g)	50
Resonance frequency (Hz)	40 k

Table 4: Technical parameters of the acceleration sensor.

Technical parameters	Parameter
Sensitivity (mv·g^{-1})	2100
Frequency range (Hz)	20~10 k
Range (g)	50
Resonance frequency (Hz)	40 k

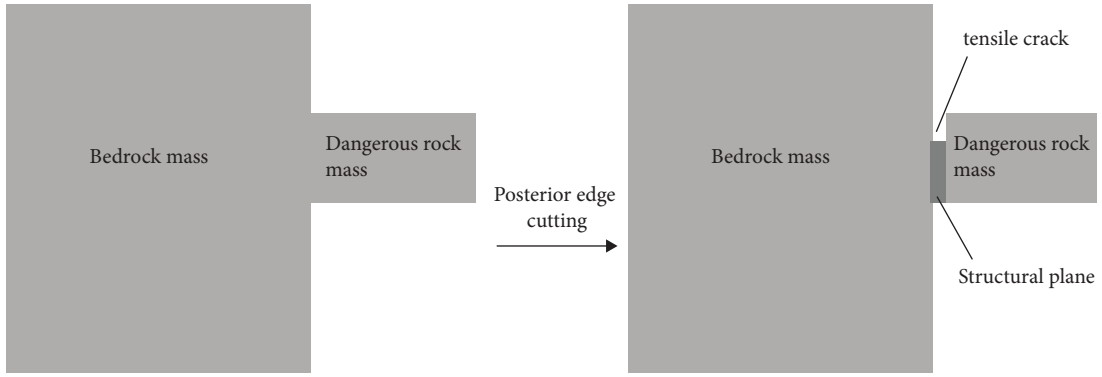

Figure 6: Diagram of a cantilevered dangerous rock mass model with cracks cut in the trailing edge.

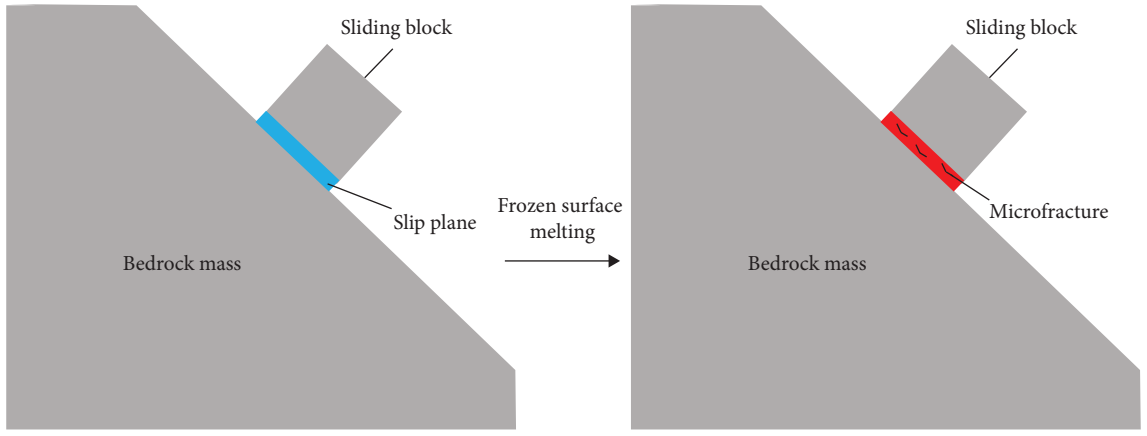

Figure 7: Diagram of freezing and melting the surface of the sliding dangerous rock mass model.

the cantilevered dangerous rock mass model [15]. During the cutting process, the data were measured and processed after each increase of 1 cm in the depth of the crack at the trailing edge of the model, and the first-order natural frequency value of the model in the Z-direction after each cut was obtained. Taking the vibration data obtained at a crack depth of 2 cm at the trailing edge of the dangerous rock mass model as an example, the frequency spectrum of the dangerous rock mass model is shown in Figure 8, the frequency spectrum of the bedrock model is shown in Figure 9, and the relative amplitude spectrum is shown in Figure 10.

As shown in Figure 10, when the crack depth at the trailing edge of the dangerous rock mass model was 2 cm, the first-order natural frequency of the dangerous rock mass was easily determined from the relative amplitude spectrum to be 399.41 Hz. The same method was used to obtain the first-

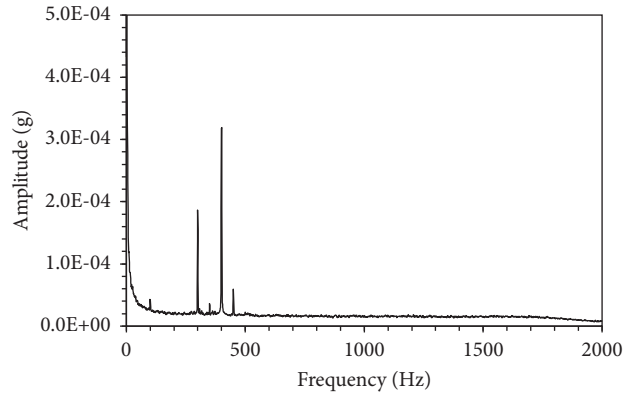

Figure 8: Spectrum of dangerous rock mass model.

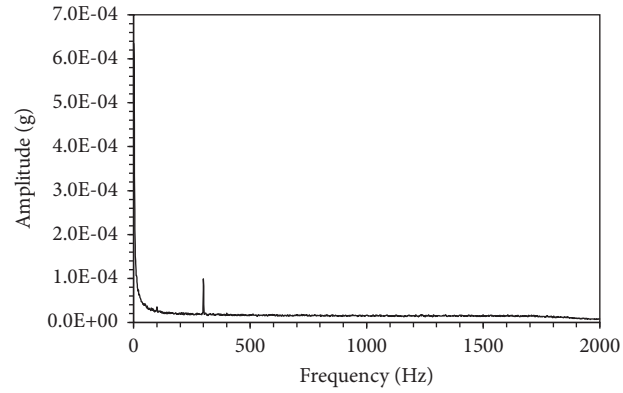

Figure 9: Spectrum of bedrock model.

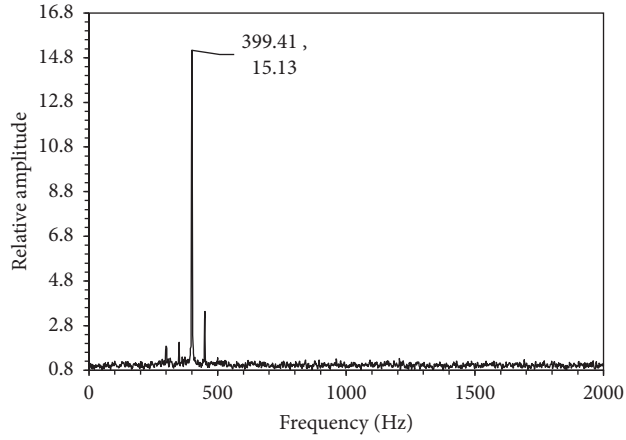

Figure 10: Relative amplitude spectrum.

order natural frequency values of the dangerous rock mass with different crack depths, as shown in Figure 11.

As shown in Figure 11, the variation of the first-order natural frequency of the cantilevered dangerous rock mass with increasing crack depth at the subsequent edge was obtained. Meanwhile, according to the model size and material parameters, the theoretical calculated value of the undamped condition was obtained by the theoretical calculation of the first-order inherent frequency of the cantilevered dangerous rock mass [15]. The theoretical calculated values of the undamped condition and the experimental measured values are shown in Figure 12.

As shown in Figure 12, the experimentally measured values for constant micromotion were basically consistent with the theoretically calculated values in the undamped condition. With increasing crack depth, the first-order natural frequency of the cantilevered dangerous rock mass showed an obvious decreasing trend, which indicated that the damage of the structural surface of the cantilevered dangerous rock mass could be identified by the first-order natural frequency. Additionally, it showed that the first-order natural frequency of the cantilevered dangerous rock mass under the condition of constant micromotion was measurable.

(2) Center Frequency. Similarly, during the cutting process, the data were measured after the depth of the crack at the trailing edge of the model increased by increments of 1 cm. The data were processed according to the method of calculating the center frequency of the dangerous rock mass. Figure 12 shows that the first-order natural frequency was always less than 650 Hz, and thus, the value of f_0 should be greater than 650 Hz. To make the change of the center of gravity frequency more obvious, f_0 cannot be too large, so f_0 was selected to be 1000 Hz for the calculation of the center frequency. The center frequency of the model after each cut is shown in Figure 13.

As shown in Figure 13, the center frequency of the dangerous rock mass remained approximately 1465 Hz throughout the experiment, and that of the bedrock basically remained approximately 1471 Hz. There was no obvious tendency for the center frequency to shift to a lower frequency. In this process, the cutting of the trailing edge of the dangerous rock mass mainly produced macroscopic cracks, and there were basically no microscopic cracks. This indicated that the macroscopic cracks in the structural face of the cantilevered dangerous rock mass could not be identified by the center frequency.

3.3.2. Sliding Dangerous Rock Mass

(1) First-Order Natural Frequency. The first-order natural frequencies in the *Y*-direction were mainly considered for the sliding dangerous rock mass model. The melting process after the freezing of the sliding dangerous rock mass lasted 25 minutes; then, one set of data was measured every minute, and a total of 26 sets of data were measured. Due to the large amount of data, the relative amplitude spectra are not listed here. According to the relative amplitude spectrum of each minute, the first-order natural frequencies of the dangerous sliding rock mass model were obtained at different times, as shown in Figure 14.

As shown in Figure 14, the first-order natural frequency of the dangerous rock mass model was maintained at approximately 137 Hz throughout the experiment. There was no significant change in the first-order natural frequency. The dangerous rock mass never destabilized during the

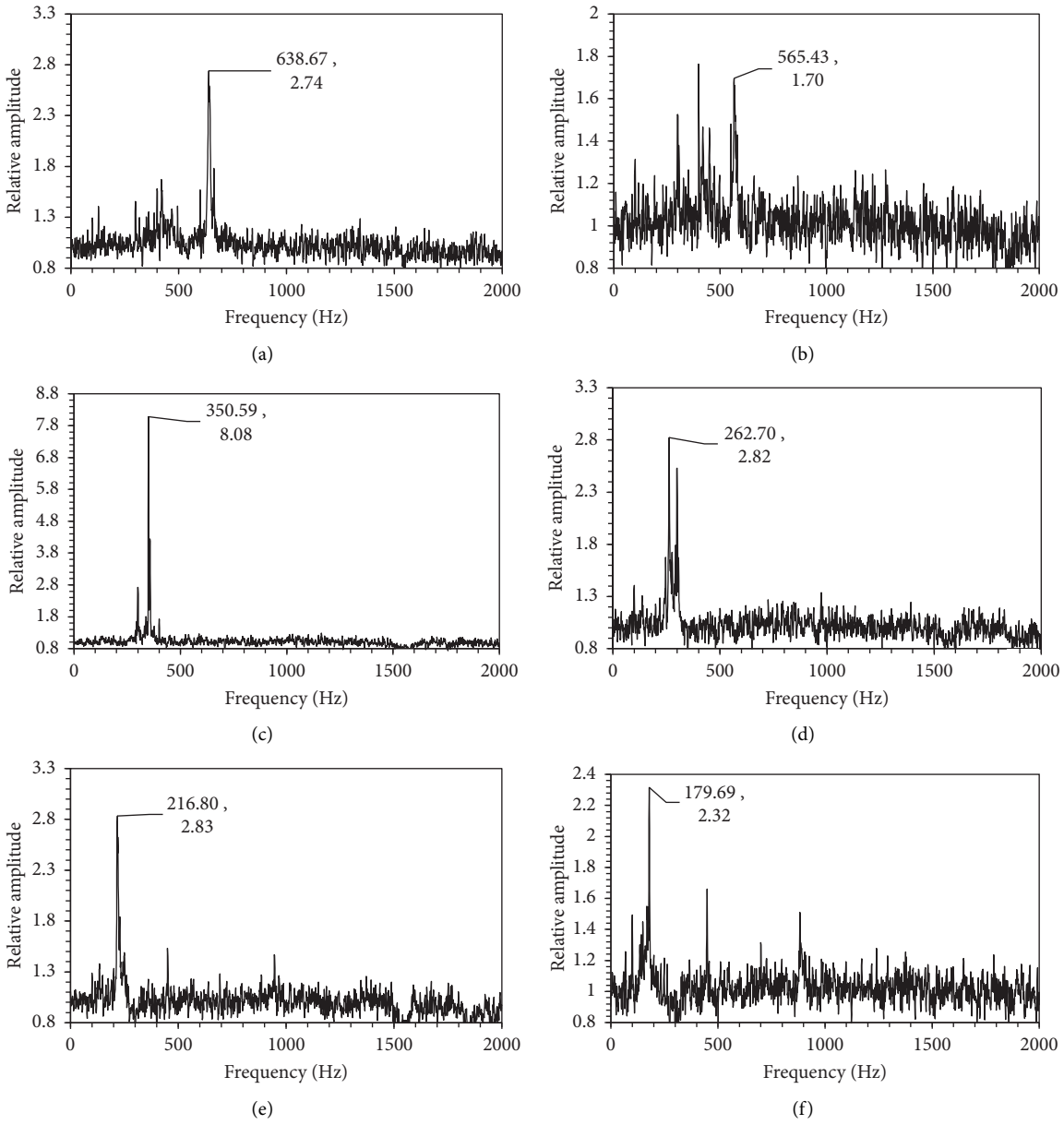

Figure 11: Relative amplitude spectra corresponding to different crack depths of the cantilevered dangerous rock mass: (a) relative amplitude spectrum when the crack depth was 0 cm, (b) relative amplitude spectrum when the crack depth was 1 cm, (c) relative amplitude spectrum when the crack depth was 3 cm, (d) relative amplitude spectrum when the crack depth was 4 cm, (e) relative amplitude spectrum when the crack depth was 5 cm, and (f) relative amplitude spectrum when the crack depth was 6 cm.

process, thus indicating that the first-order natural frequency was not sensitive to the damage caused by the microscopic fractures. In addition, the displacement, which is an indicator of deformation of the dangerous rock mass in this process, failed.

(2) Center Frequency. The curves of the changes in the center frequency values of the dangerous rock mass model and the bedrock model with increasing melting time of the frozen surface are shown in Figure 15.

As shown in Figure 15, the center frequencies of both the dangerous sliding rock mass and its bedrock decreased during the first 10 minutes. This was because the structure medium was damaged with the melting of the frozen surface.

The decrease in the center frequency of the bedrock was greater than that of the dangerous rock mass. The reason was that the elastic wave propagated from the bedrock to the dangerous rock mass through the structural surface with fissures, then reflected back from the critical boundary of the dangerous rock mass to the bedrock, and passed through the structural surface with fissures again. The high-frequency part of the elastic wave measured at the bedrock was attenuated twice, while the high-frequency part of the elastic wave at the dangerous rock mass was only attenuated once, as shown in Figure 16.

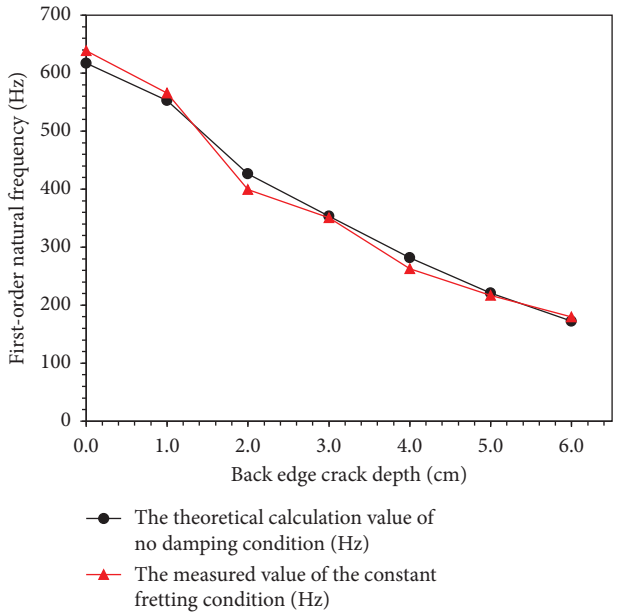

Figure 12: First-order natural frequency variation curve of the cantilever dangerous rock mass model.

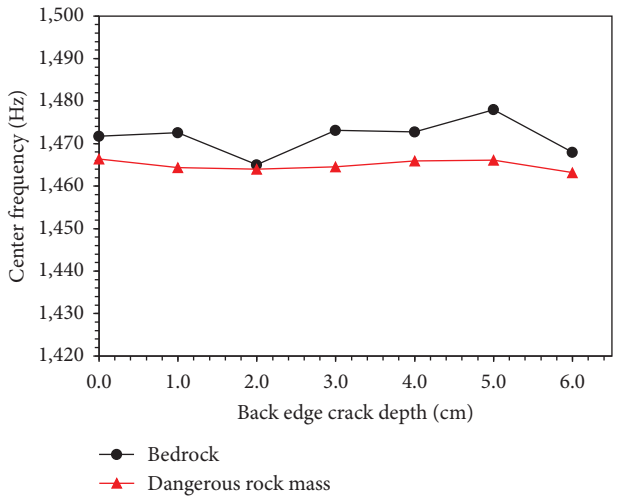

Figure 13: Center frequency variation curve of the cantilever dangerous rock mass and its bedrock.

Within the 10th~15th minute, the microscopic fractures continued to increase as the frozen surface continued to melt. At the same time, the dangerous rock mass model was continuously fitted to the bedrock model, and the state of the dangerous rock mass model was continuously adjusted. The center frequency fluctuated. In the 15th~25th minute, the freezing surface gradually melted completely, the dangerous rock mass model was completely fitted to the bedrock model, and the microscopic fissures were gradually closed, leading to the rebound of the center frequency.

The experimental phenomena showed that the damage of the surface of the structure by microfractures of the

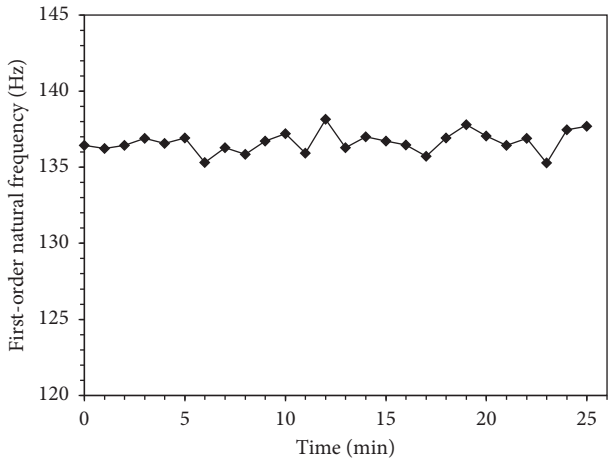

Figure 14: Relative amplitude ratio of the slip dangerous rock mass model.

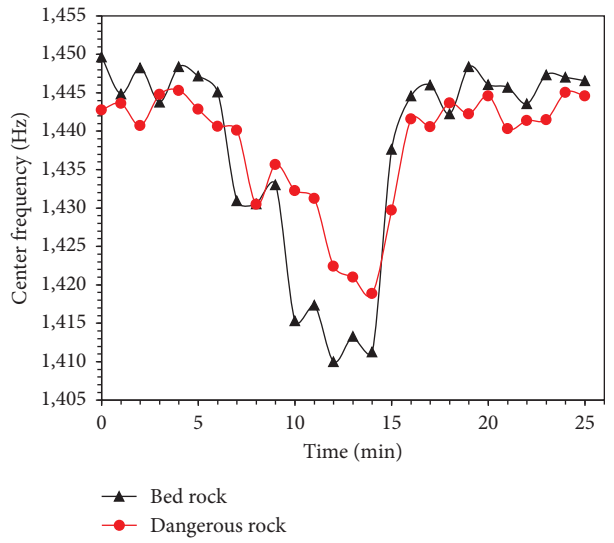

Figure 15: Variation of the center frequencies of the slip dangerous rock mass and its bedrock.

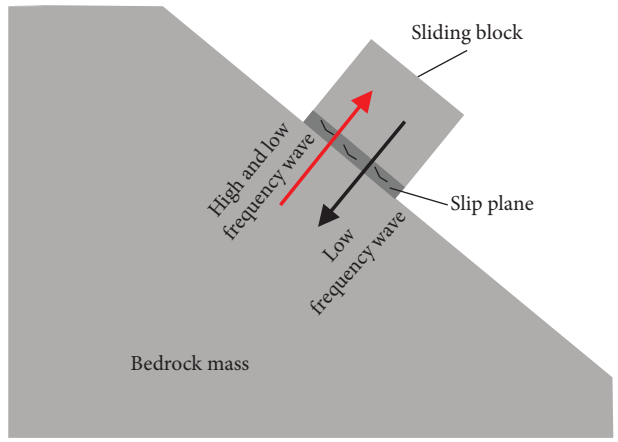

Figure 16: Elastic wave propagation process.

sliding dangerous rock mass could not be reflected significantly based on the first-order natural frequency. Instead, the development of its fractures could be reflected by the trend of its center frequency change, and then, the change in its damage degree could be identified. In addition, the dangerous rock mass did not slip at all times during the experiment, which indicated the limitation of using the displacement index to reflect the damage of the face of the structure.

4. Discussion

4.1. Difference between the Dynamic Characteristics of the Dangerous Rock Mass and Those of the Site. Site micromotions contain information on site characteristics, and their remarkable frequencies can reflect the dynamic characteristics of the overburden and the site [38]. Theoretically, constant micromotion data can reveal the characteristics of the stratigraphy where the site is located. However, due to the inhomogeneity of the geological mass, the complexity of the stratigraphic system and the geometric characteristics of the site, and the unknown and random nature of the geotechnical physical properties, the remarkable frequency can only roughly reflect the dynamic characteristics of the site. It is difficult to determine the local dynamic characteristics of the site based on the propagation law of elastic waves in the strata [39]. The dangerous rock mass-bedrock system is localized with respect to the site, and its dynamic characteristics are often not fully consistent with the site as a whole. Therefore, the variation in the dangerous rock mass vibration distribution in different frequency bands is closely related to the degree of structural surface damage and almost unrelated to the dynamic characteristics of the site.

4.2. Application Method of the Dynamic Index of the Dangerous Rock Mass. Based on the experimental results, the trends of the first-order natural frequencies and center frequencies were obtained for dangerous rock masses controlled by macroscopic fractures and those controlled by microscopic fractures. The first-order natural frequencies of the dangerous rock masses controlled by macroscopic fracture were more sensitive to changes in damage of the surface structure, and the center frequencies were less sensitive. In contrast, the center frequencies of dangerous rock masses controlled by microscopic fracture were more sensitive to changes in structural surface damage, and the first-order natural frequency was less sensitive. The main reason for this phenomenon was that the damage of the dangerous rock mass with macroscopic fracture was the generation of macroscopic fracture under the compound action of tension and shear. The generation of macroscopic fractures changed the geometric characteristics and boundary conditions of the dangerous rock mass. With the increase in macroscopic fracture depth at the back edge of the dangerous rock mass, the constraint area of bedrock on the dangerous rock mass decreased, and the position of the constraint also changed. Therefore, the first-order natural frequency of the dangerous rock mass controlled by macroscopic fracture decreased significantly with increasing macroscopic fracture depth of the surface structure. For the dangerous rock mass controlled by microscopic fracture, the dangerous rock mass and the bedrock basically remained in a state of advection before imminent damage. The structural surface often did not show macroscopic fracture. That is, the bedrock constraint area and action position of the dangerous rock mass were basically unchanged, and its first-order natural frequency also remained basically unchanged. Macroscopic fractures and microscopic fractures were not antagonistic, macroscopic fractures intensified the formation of microscopic fractures, and the expansion and penetration of microscopic fractures eventually formed macroscopic fractures. Based on the relationship between macroscopic fractures and microscopic fractures and the corresponding dynamic characteristics of the dangerous rock mass, the author believes that the first-order natural frequency index and the center frequency index should be used to discern the current state of a dangerous rock mass to comprehensively reflect the changes in the degree of damage of the surface structure of the dangerous rock mass.

In addition, the experimental results of the model of the dangerous sliding rock mass showed that the displacement index did not comprehensively reflect the change in the degree of damage of the structural face, but the center frequency value appeared to significantly change. This reflected the validity of the identification of the change in the degree of damage of surface structure based on the dynamic index.

5. Conclusions

This paper studied the first-order natural frequency identification method and the principle of calculating the center frequency of a dangerous rock mass with a single surface structure under the condition of constant micromotion and conducted indoor experiments. Experiments were conducted to study the dynamic characteristics of two models of dangerous rock masses with a single surface structure, cantilevered dangerous rock mass, and sliding dangerous rock mass. The main conclusions are as follows:

(1) Based on the theory of vibration mechanics, the relative amplitude spectrum of the dangerous rock mass and the bedrock was proposed. Based on the relative amplitude spectrum, the first-order natural frequency of the dangerous rock mass could be obtained, and the measurability of the first-order natural frequency of the dangerous rock mass under the condition of constant micromotion was proven through experiments.

(2) The structural surface damage of macroscopic fracture-controlled dangerous rock masses could be identified by the first-order natural frequency of the dangerous rock masses, but the damage could not be reflected by the center frequency. The structural surface damage of microscopic fracture-controlled dangerous rock masses could be identified by the

change in the center frequency in its high-frequency band, but the damage could not be reflected by the first-order natural frequency.

(3) For a dangerous rock mass with a single surface structure, the use of only vibration mechanics theory or elastic wave scattering theory to analyze the damage of a dangerous rock mass structural surface had limitations. The combination of both theories will be more effective to identify the damage of the surface structure of dangerous rock masses.

In this paper, the damage of the surface structure of dangerous rock masses controlled by macroscopic and microscopic damage was qualitatively analyzed by dynamic characteristics. In a subsequent study, the author will continue to study the quantitative relationship between the change in dynamic characteristics and the degree of damage of surface structure of the two kinds of dangerous rock masses in detail.

Data Availability

The data supporting the current study are available from the corresponding author upon request.

Conflicts of Interest

The authors declare that they have no conflicts of interest.

Acknowledgments

This work was supported by the Key Science and Technology Plan Project of PowerChina Huadong Engineering Corporation Limited (Grant No. KY2021-ZD-03).

References

[1] M. S. Diederichs, "Manuel rocha medal recipient rock fracture and collapse under low confinement conditions," *Rock Mechanics and Rock Engineering*, vol. 36, no. 5, pp. 339–381, 2003.

[2] Y. M. Liu and C. C. Xia, "Study on fracture mechanism and criteria of failure strength of rock mass containing coplanar close discontinuous joints under direct shear," *Chinese Journal of Rock Mechanics and Engineering*, no. 10, pp. 2086–2091, 2006.

[3] Y. Du, *Study on the Model of Rock Block Stability Evaluation Based on Natural Vibration Frequency*, University of Science and Technology Beijing, Beijing, China, 2016.

[4] A. Kyriou, K. Nikolakopoulos, I. Koukouvelas, and P. Lampropoulou, "Repeated UAV campaigns, GNSS measurements, GIS, and petrographic analyses for landslide mapping and monitoring," *Minerals*, vol. 11, no. 3, p. 300, 2021.

[5] I. Kulsoom, W. Hua, S. Hussain, Q. Chen, G. Khan, and D. Shihao, "SBAS-InSAR based validated landslide susceptibility mapping along the Karakoram Highway: a case study of Gilgit-Baltistan, Pakistan," *Scientific Reports*, vol. 13, no. 1, p. 3344, 2023.

[6] M. J. Stumvoll, E. M. Schmaltz, and T. Glade, "Dynamic characterization of a slow-moving landslide system – a," *Geomorphology*, vol. 389, Article ID 107803, 2021.

[7] H. Yang, L. W. Wang, and S. W. Hao, "Landslide monitoring and its stabilization process based on an in-situ tilt monitoring system [J]," *Engineering Mechanics*, vol. 37, no. 1, pp. 193–199, 2020.

[8] F. M. Huang, P. Wu, and Y. Y. Ziggah, "GPS monitoring landslide deformation signal processing using time-series model," *International Journal of Signal Processing, Image Processing and Pattern Recognition*, vol. 9, no. 3, pp. 321–332, 2016.

[9] L. G. Gao, T. Li, X. Liu et al., "A novel dynamic stability analysis method for jointed rock slopes based on block-interface interaction," *Computers and Geotechnics*, vol. 134, Article ID 104113, 2021.

[10] D. d'Angiò, L. Lenti, and S. Martino, "Microseismic monitoring to assess rock mass damaging through a novel damping ratio-based approach," *International Journal of Rock Mechanics and Mining Sciences*, vol. 146, Article ID 104883, 2021.

[11] W. Zhang, N. Ma, J. Ren, and C. Li, "Peak particle velocity of vibration events in underground coal mine and their caused stress increment," *Measurement*, vol. 169, Article ID 108520, 2021.

[12] B. Jia, Z. Wu, and Y. Du, "Real-time stability assessment of unstable rocks based on fundamental natural frequency," *International Journal of Rock Mechanics and Mining Sciences*, vol. 124, Article ID 104134, 2019.

[13] J. Wasowski, M. J. Mcsaveney, L. Pisano, V. Del Gaudio, Y. Li, and W. Hu, "Recurrent rock avalanches progressively dismantle a mountain ridge in Beichuan County, Sichuan, most recently in the 2008 Wenchuan earthquake," *Geomorphology*, vol. 374, Article ID 107492, 2021.

[14] Y. Du, M. W. Xie, and J. Y. Jiang, "Research progress on dynamic monitoring index for early warning of rock collapse [J]," *Chinese Journal of Engineering*, vol. 41, no. 4, pp. 427–435, 2019.

[15] X. Y. Zhang, M. W. Xie, and L. Zhang, "Study on calculation model of stability cofficient of falling dangerous rock mass based on natural frequency," *[J]. Chinese Journal of Rock Mechanics and Engineering*, pp. 1–9, 2022.

[16] X. Y. Zhang, M. W. Xie, and L. Zhang, "A calculation model of safety factor of shear fractured falling dangerous rock mass based on natural frequency," *Journal of Engineering Mechanics*, vol. 39, pp. 1–11, 2022.

[17] M. Xie, W. Liu, Y. Du, Q. Li, and H. Wang, "The evaluation method of rock mass stability based on natural frequency," *Advances in Civil Engineering*, vol. 2021, Article ID 6652960, 9 pages, 2021.

[18] P. Bottelin, L. Baillet, E. Larose et al., "Monitoring rock reinforcement works with ambient vibrations: La Bourne case study (Vercors, France)," *Engineering Geology*, vol. 226, pp. 136–145, 2017.

[19] W. N. Liu, *Study on the Stability Dynamics Evaluation Model of Falling Dangerous Rock Masses on Slope*, University of Science and Technology, Beijing, China, 2022.

[20] N. Chatzis, C. Papazachos, N. Theodoulidis et al., "Metamorphic bedrock geometry of Santorini using HVSR information and geophysical modeling of ambient noise and active-source surface-wave data," *Journal of Volcanology and Geothermal Research*, vol. 432, Article ID 107692, 2022.

[21] S. Molnar, A. Sirohey, J. Assaf et al., "A review of the microtremor horizontal-to-vertical spectral ratio (MHVSR) method," *Journal of Seismology*, vol. 26, no. 4, pp. 653–685, 2022.

[22] C. Zhu, M. Pilz, and F. Cotton, "Which is a better proxy, site period or depth to bedrock, in modelling linear site response

in addition to the average shear-wave velocity? [J]," *Bulletin of Earthquake Engineering*, vol. 18, no. 3, pp. 797–820, 2020.

[23] L. B. Zhang, W. L. Shen, X. L. Li et al., "Abutment pressure distribution law and support analysis of super large mining height face," *International Journal of Environmental Research and Public Health*, vol. 20, no. 1, p. 227, 2022.

[24] X. L. Li, X. Y. Zhang, W. L. Shen et al., "Research on the mechanism and control technology of coal wall sloughing in the ultra-large mining height working face," *International Journal of Environmental Research and Public Health*, vol. 20, no. 1, p. 868, 2023.

[25] J. C. Zhang, X. L. Li, Q. Qin, Y. Wang, and X. Gao, "Study on overlying strata movement patterns and mechanisms in super-large mining height stopes," *Bulletin of Engineering Geology and the Environment*, vol. 82, no. 4, p. 142, 2023.

[26] L. Qian and S. Zang, "Differentiation rule and driving mechanisms of collapse disasters in changbai county," *Sustainability*, vol. 14, no. 4, p. 2074, 2022.

[27] Y. Chen, P. Wu, and Q. Yu, "Effects of freezing and thawing cycle on mechanical properties and stability of soft rock slope," *Advances in Materials Science and Engineering*, vol. 3, 2017.

[28] G. Chen, Y. Wan, Y. Li, X. Pei, and D. Huang, "Time-dependent damage mechanism of rock deterioration under freeze–thaw cycles linked to alpine hazards," *Natural Hazards*, vol. 108, no. 1, pp. 635–660, 2021.

[29] C. Shi, B. Yang, Y. Zhang et al., "Application of discrete-element numerical simulation for calculating the stability of dangerous rock mass: a case study [J]," *International Journal of Geomechanics*, vol. 20, no. 12, Article ID 04020231, 2020.

[30] J. Valentin, A. Capron, D. Jongmans et al., "The dynamic response of prone-to-fall columns to ambient vibrations: comparison between measurements and numerical modelling," *Geophysical Journal International*, vol. 208, no. 2, pp. 1058–1076, 2016.

[31] D. J. Jwo, W. Y. Chang, and I. H. Wu, "Windowing techniques, the welch method for improvement of power spectrum estimation," *CMC-Computers Materials and Continua*, vol. 67, 2021.

[32] J. A. Hudson, "Wave speeds and attenuation of elastic waves in material containing cracks," *Geophysical Journal International*, vol. 64, no. 1, pp. 133–150, 1981.

[33] T. Pointer, E. Liu, and J. A. Hudson, "Seismic wave propagation in cracked porous media," *Geophysical Journal International*, vol. 142, no. 1, pp. 199–231, 2000.

[34] E. Liu, J. H. Queen, Z. Zhang, and D. Chen, "Simulation of multiple scattering of seismic waves by spatially distributed inclusions," *Science in China - Series E: Technological Sciences*, vol. 43, no. 4, pp. 387–394, 2000.

[35] S. M. Liu and X. L. Li, "Experimental study on the effect of cold soaking with liquid nitrogen on the coal chemical and microstructural characteristics," *Environmental Science and Pollution Research*, vol. 30, no. 13, pp. 36080–36097, 2022.

[36] S. M. Liu, H. T. Sun, D. M. Zhang et al., "Nuclear magnetic resonance study on the influence of liquid nitrogen cold soaking on the pore structure of different coals," *Physics of Fluids*, vol. 35, no. 1, Article ID 012009, 2023.

[37] S. M. Liu, H. T. Sun, D. M. Zhang et al., "Experimental study of effect of liquid nitrogen cold soaking on coal pore structure and fractal characteristics," *Energy*, vol. 275, no. 7, Article ID 127470, 2023.

[38] S. M. T. Qadri and O. A. Malik, "Establishing site response-based micro-zonation by applying machine learning techniques on ambient noise data: a case study from Northern Potwar Region, Pakistan," *Environmental Earth Sciences*, vol. 80, pp. 1–15, 2021.

[39] J. S. Bo, X. L. Li, and Z. Y. Li, "Some progress of study on the effect of site condtion on ground motion," *WORLD EARTHOUAKE ENC NEERING*, no. 2, pp. 11–15, 2003.